Orbital dynamics and characterization of space debris via optical observations

Hager GHONIEM[1], Mohamed RADWAN*[,1], Hany DWIDAR[1],
Yehia ABDEL-AZIZ[2], Ahmed Magdy ABDEL-AZIZ[2]

*Corresponding author
*[,1]Department of Astronomy and Space science, Faculty of Science,
Cairo University, Egypt,
mradwan@sci.cu.edu.eg
[2]National Research Institute of Astronomy and Geophysics,
Helwan, 11421, Cairo, Egypt

Abstract: Studying the long-term dynamical evolution of space debris and the development of optical measurements help us to avoid collision risks caused by these objects. In this work we studied the long-term evolution of space debris orbits, in GEO and MEO regions, under the effect of natural perturbations. The perturbations considered are the Earth's gravitational field, luni-solar attraction and solar radiation pressure as well. To characterize and track the space debris we used the optical space surveillance system (OSTS) constructed by the National Research Institute of Astronomy and Geophysical (NRIAG). To better understanding the long-period dynamics we carried out several numerical explorations on space debris with small area-to-mass ratio (between $0.009 m^2/kg$ and $0.09 m^2/kg$). We found that zonal potential and solar radiation pressure play an important role in the dynamics of the problem.

Key Words: Space debris, Optical measurements, Long-term dynamics, Collision, Perturbation

1. INTRODUCTION

The space surrounding planet Earth is densely populated by an increasing number of man-made space debris, the origin of these objects is attributed to the break-up of operational artificial satellites, upper stages of launchers or abandoned spacecraft. These space objects are recognized as a hazard to current and even for future space activities because the probability of collision between a spacecraft and space debris is real ([1], [2], [3], [4]). Consequently, the study of the long-term dynamical evolution of space debris is essential to know the behavior of the population in the future. Also, investigating the orbital dynamics of space debris through different techniques allow a deeper insight into the orbit debris evolution under the combined effect of natural perturbations ([5], [3]).

Space debris on high altitudes are subjected to several perturbations and their interactions, including the Earth's gravitational field, luni-solar perturbations and solar radiation pressure. Thus, their dynamical evolution is complicated ([6]). The current analytical model neglects the effect of the tesseral harmonics, since at high altitude orbits, the terms due to tesseral harmonics are two orders of magnitude smaller than the other perturbations (see [7]).

As aforementioned, space debris are a risk for the space operations. The debris pieces are a threat due to their high relative velocity with respect to other objects in orbit. Thus, the optical systems became crucial for any country to track and characterize debris in order to curtail the possibility of collision between debris and operational artificial satellites.

The passive optical observations scheme uses the fact that orbital objects are illuminated by the sun, while the sky background is dark, and reflect part of the sunlight to the observer on the ground. This type of observations are cheap and can yield precise information about the apparent position of the debris via comparison with background stars ([8], [9], [10], [11], [12], [13]).

The long-term dynamics of space debris orbits under the influence of different perturbations was extensively studied. This allowed obtaining insightful information about evolution under the effect of perturbations. Many analytical and semi-analytical studies of these space objects at different altitude orbits have been developed by several authors. Some researchers have focused their attention on space debris, with high area-to mass ratio, orbiting in the geosynchronous region and the Earth shadowing effects (see [14], [15], [16], [17], [18], [5]). Other researchers focused on the analysis of the resonant problem [14]. In this paper, we continue the previous efforts made by researchers to study the dynamical evolution of the space debris to avoid its risks. We used the optical surveillance system (OSTS) constructed by NRIAG to track and identify space debris at high altitude orbits, especially in the GEO and MEO regions. We investigated the long-term dynamics of space debris under the effects of earth's gravitational field, luni-solar attraction and solar radiation pressure as well.

2. OPTICAL OBSERVATIONS

High altitude Earth orbits, in particular Geosynchronous (GEO) orbits, are crowded by space missions. So that the risk of a collision between space debris and an active satellites is not negligible. Consequently, dedicated observation schemes are in operation globally to detect debris and study their orbital evolution. Passive optical observations are used to detect new space objects and to track and further characterize known objects. Currently, the number of debris estimated by statistical models are more than 34,000 object larger than 10 cm in diameter. These tracked objects mainly consist of expended rocket bodies and fragments from spacecraft breakups ([8], [12], [13]).

Similar to the planets, comets and minor planets in the solar system, near-earth space debris moves with respect to the background stars, and hence there is a relative movement between space debris and background stars during exposure. CCD images are obtained as the process for tracking space objects is applied, and for Geosynchronous Orbit objects, which move slowly with respect to the stars, the drive is turned off during exposure. Such a strategy shows the images of objects of interest as points, while the background stars appear as streaks ([10].

In order to curtail the risks caused by space debris, the National Research Institute of Astronomy and Geophysical (NRIAG) constructed an optical space surveillance system (OSTS) at 29.933° N, 31.8823° E and 470 m above sea level. This system is a passive optical tracking unit for tracking and detecting space objects orbiting the Earth at different altitudes. The system consists of Celestron 11″ Rowe-Ackermann Schmidt Astrograph with a focal plane that is 70 mm in diameter and CGE Pro Computerized/Motorized EQ Mount (see table 1). The software of OSTS divided into two parts, the first part contains some collection windows-based software for mount and camera control and the second part is astronomical image processing software [8].

Table 1: Optical Satellites Tracking Station (OSTS) components

Items	Characteristics
Telescope Series	Celestron 11″ Rowe-Ackermann Schmidt Astrograph with CGE Pro Mount
Telescope Aperture	11″
Telescope Focal Ratio	f/2.2
Telescope Focal Length	620 (mm)
Focuser Style	Internal Moving Primary
Focuser Speed	Dual Speed
Telescope Mount Type	Equatorial
CCD device	MicroLine ML11002 Monochrome Camera Grade 2
Pixels	4072 × 2720 pixels
Pixel Size (μm)	9.0 × 9.0
Cooling	Peltier 55 °C below ambient Temperature
Interface	USB 2.0
System (FOV)	3.4° × 2.3°
PC	Two PC core I7

Using the above mentioned optical tracking system we detected three space debris. The positional and photometric measurements of these space objects are performed by the universal software package Apex-II ([19]). After initial orbit determination we found that these three objects are known space debris and cataloged in NORAD two-line element set as shown in Table 2.

Table 2 – The two-line element set of the detected space objects

Name of debris	Semi major axis km	Eccentricity	Inclination deg.	RA ascend. node deg.	Arg. of perigee deg.	Mean anomaly deg.	Mean motion
BREEZE-M R/B	38678.878	0.0704063	3.980	78.857	119.175	227.237	1.1412794
ARIANE 5 DEB (SYLDA)	18843.554	0.7206023	4.553	5.259	224.493	259.315	3.3562828
ATLAS AGENA D R/B	37025.652	0.1001541	4.146	293.727	334.450	176.408	1.2185650

3. DYNAMICAL MODEL

Space objects at high altitude Earth orbits experience a complex and dynamic set of perturbations, such as the Earth's oblateness, third-body gravity perturbations and solar radiation pressure. Let us describe the motion of space debris using a set of orbital elements $(a, e, i, \omega, \Omega, \tau)$. Where a is the semi-major axis, e is the eccentricity, i is the inclination, ω is the argument of perigee, Ω is the longitude of the ascending node and τ is the time of periapsis passage. This set of orbital elements is referenced to the Earth-centered inertial reference frame. In what follows we will mention briefly the involved perturbing forces.

3.1 Earth's potential

Taking into account the Earth's gravitational field is essential when studying the motion of space objects orbiting the Earth. This due to the fact that Earth is not a spherically symmetric body but is bulged at the equator, flattened at the poles and is generally asymmetric ([20]).

The Earth`s gravity potential can be written as ([21])

$$U = \frac{\mu}{r} \sum_{n=0}^{\infty} \sum_{m=0}^{n} \left(\frac{R_E}{r}\right)^n P_{nm} (\sin \varphi) (C_{nm} \cos m\lambda + S_{nm} \sin m\lambda) \tag{1}$$

where μ is the gravitational parameter of the earth, R_E its equatorial radius and r is the distance of the space debris from the earth. J_n are the coefficients that characterize the size of non-spherical component of the potential. The angle φ is the geocentric latitude and λ is the longitude. P_{nm} are Legendre polynomials of degree n and order m. The quantities C_{nm} and S_{nm} are the known tesseral harmonics. When $m = 0$ the potential function including the zonal harmonic coefficients effect J_n can be written as

$$U = \frac{\mu}{r} + R \tag{2}$$

$$R = -\frac{\mu}{r} \sum_{n=2}^{\infty} J_n \left(\frac{R_E}{r}\right)^n P_n (\sin \varphi) \tag{3}$$

To obtain a simplified dynamical system we carry out an averaging process to remove the fast-rotating variables from the disturbing potential. To reduce the degrees of freedom of the system we average the potential over the mean anomaly of the space object, then the normalized zonal potential may be written in terms of the orbital elements as ([4])

$$R_z = \frac{R_E^2 J_2 \mu}{a^3(1-e^2)^{3/2}} \left(\frac{-1}{2} + \frac{3 sin^2 i}{4}\right) + \frac{2 e R_E^3 J_3 \mu \sin \omega}{a^4(1-e^2)^{5/2}} \left(-\frac{3 sin^2 i}{4}\right.$$
$$\left. + \frac{15 sin^3 i}{16}\right) + \frac{R_E^4 J_4 \mu}{a^5(1-e^2)^{7/2}} \left[\frac{3 e^2 \sin 2\omega}{2} \left(\frac{15 sin^2 i}{16} - \frac{35 sin^4 i}{32}\right)\right. \tag{4}$$
$$\left. + \left(1 + \frac{3e^2}{2}\right) \left(\frac{3}{8} - - \frac{15 sin^2 i}{8} - \frac{105 sin^4 i}{64}\right)\right]$$

where $\sin \varphi = \sin i \, \sin(\omega + f)$.

3.2 Third body attraction

For high-altitude Earth orbits, the third body plays a crucial role in the dynamics of the problem, it exerts a large perturbation and sometimes dominates the dynamic. The influence of third body attraction on a space object is usually modeled as a series expansion of the potential w.r.t the ratio between the semi-major axis and the distance to the third body ([22]). The potential function due to the attraction of the third body may be written as ([23])

$$U_{3b} = \mu_1 \left(\frac{1}{\|\bar{r} - \bar{r}_1\|} - \frac{\bar{r}.\bar{r}_1}{\bar{r}_1{}^3}\right) \tag{5}$$

where μ_1 represents the gravitational parameter of the third body. $\bar{r}$ and $\bar{r}_1$ are the radius vectors of the debris and the third body with respect to the main body, respectively. Since we are interested in the case $r \ll r_1$, the term $\frac{1}{\|\bar{r}-\bar{r}_1\|}$ is expanded as a series of Legendre polynomials up to order two. Hence

$$\frac{1}{\|\bar{r} - \bar{r}_1\|} = \frac{1}{r_1} (1 - 2\left(\frac{r}{r_1}\right)\cos s + \left(\frac{r}{r_1}\right)^2)^{\frac{1}{2}} \tag{6}$$

$$\frac{1}{\|\bar{r} - \bar{r}_1\|} = \frac{1}{r_1} \sum_{n \geq 0}^{2} \left(\frac{r}{r_1}\right)^n P_n(\cos s) \tag{7}$$

where s is the angle between the two radius vectors $\bar{r}$ and $\bar{r}_1$. Replacing the expression of the Legendre polynomials, $P_0(\cos s) = 1$, $P_1(\cos s) = \cos s$ and $P_2(\cos s) = (-1 + 3\cos^2 s)/2$, we have

$$U_{3b} = \frac{\mu_1}{r_1}[\,1 + \frac{1}{2}\left(\frac{r}{r_1}\right)^2 (3\cos^2 s - 1)] \tag{8}$$

Carrying out a two-fold averaging process to remove the mean anomalies of the debris and the third body, in succession, then the double-averaged potential due to the luni-solar attraction may be written as ([24])

$$
\begin{aligned}
R_s = \; n_s^2\, a^2 \; \bigg[& \Big\{\Big(1 + \frac{3}{2}e^2\Big)\Big]\Big\{\frac{1}{4}\,(1 - \frac{3}{2}\sin^2 i)\Big(1 - \frac{3}{2}\sin^2 i_s\Big) \\
& + \frac{3}{16}\sin 2i\,\sin 2i_s\,\cos\Omega + \frac{3}{16}\sin^2 i\,\sin^2 i_s\cos 2\Omega\Big\} \\
& + \frac{15e^2}{8}\Big\{\frac{1}{2}\sin^2 i\Big(1 - \frac{3}{2}\sin^2 i_s\Big)\cos 2\omega \\
& + \frac{1}{2}\cos^4\frac{i}{2}\sin^2 i_s\,\cos 2(\omega + \Omega) \\
& - \frac{1}{2}\,\sin i\,\cos^2\frac{i}{2}\,\sin 2i_s\cos(2\omega + \Omega) + \frac{1}{2}\,\sin^4 i\,\sin^2 i_s\cos 2(\omega \\
& - \Omega) + \frac{1}{2}\sin i\,\sin^2\frac{i}{2}\sin 2i_s\,\cos(2\omega - \Omega)\Big\}\bigg]
\end{aligned} \tag{9}
$$

and

$$
\begin{aligned}
R_M = \; n_m^2\,\mu_m\,a^2\;\bigg[& \Big\{\Big(1 + \frac{3}{2}e^2\Big)\Big]\Big\{\frac{1}{4}\,(1 - \frac{3}{2}\sin^2 i)\Big(1 - \frac{3}{2}\sin^2 i_m\Big) \\
& + \frac{3}{16}\sin 2i\,\sin 2i_m\,\cos(\Omega - \Omega_m) \\
& + \frac{3}{16}\sin^2 i\,\sin^2 i_m\cos 2(\Omega - \Omega_m)\Big\} \\
& + \frac{15e^2}{8}\Big\{\frac{1}{2}\sin^2 i\Big(1 - \frac{3}{2}\sin^2 i_m\Big)\cos 2\omega \\
& + \frac{1}{2}\cos^4\frac{i}{2}\sin^2 i_m\,\cos 2(\omega + \Omega - \Omega_m) \\
& - \frac{1}{2}\,\sin i\,\cos^2\frac{i}{2}\,\sin 2i_m\cos(2\omega + \Omega - \Omega_m) \\
& + \frac{1}{2}\,\sin^4 i\,\sin^2 i_m\cos 2(\omega - \Omega + \Omega_m) \\
& + \frac{1}{2}\sin i\,\sin^2\frac{i}{2}\sin 2i_m\,\cos(2\omega - \Omega + \Omega_m)\Big\}\bigg]
\end{aligned} \tag{10}
$$

where R_s and R_M are the disturbing potentials due to Sun and Earth, respectively. $\mu_m = 1/82.3$ is the ratio between the mass of the Moon and the sum of the masses of the Earth and the Moon; $n_s = 0.017203$ rad/day is the Sun's apparent orbit mean motion; $n_m = 0.23$ rad/day is the Moon's orbit mean motion; i_m is the Moon's orbit inclination to the equatorial plane; Ω_m is the right ascension of the ascending node of the Moon's orbit with respect to the equator; and $i_s = 23.445°$ is the Sun's apparent orbit inclination to the equatorial plane. As it is known, due to the lunar regression the two angles i_m and Ω_m vary with time.

3.3 Solar radiation pressure

Solar radiation pressure is a non-conservative force that becomes more pronounced at higher altitude orbits. For objects with exceptionally high area-to-mass ratios, the solar radiation pressure perturbation may lead to highly eccentric orbits ([25]). The normalized disturbing potential due to radiation pressure, averaged over the orbital motion of the space object, may be written in the form ([26])

$$R_{SRP} = \frac{3}{2} P \, C_R \, \frac{A}{m} \, a \, e[\cos \omega(\cos \Omega \cos \lambda_S \, \cos \epsilon + \sin \Omega \sin \lambda_S \, \cos \epsilon)$$
$$+ \sin \omega(\cos \Omega \cos i \sin \lambda_S \, \cos \epsilon - \sin \Omega \cos i \cos \lambda_S)$$
$$+ \sin \omega \sin i \sin \lambda_S \, \sin \epsilon] \tag{11}$$

where $A/M = \beta$ is the area-to-mass ratio, ϵ is the obliquity of the ecliptic, λ_S is the longitude of the Sun measured on the ecliptic plane, P the solar radiation pressure and C_R the reflectivity coefficient.

4. NUMERICAL SIMULATION AND CONCLUSIONS

The averaged disturbing potential of the orbital motion of space debris taking into consideration the gravitational attraction of the Earth, the luni-solar attraction and the solar radiation pressure are given by equations (4), (9), (10) and (11). To analyze their effects on the orbital elements of the observed three objects, this potential is substituted into Lagrange's planetary equations. In order to observe how the area to mass ratio A/M influences the orbital evolution of detected space debris in GEO and MEO regions, we carried out a series of numerical simulations on objects with A/Ms ranging from 0.009 m^2/kg to 0.09 m^2/kg. The long-term numerical integrations for inclination and orbital eccentricity are performed up to 100 years. The estimated range of the A/M values of the space debris in that region is about $2 \times 10^{-3} - 2 \times 10^{-2} m^2/kg$, ([27]). Results from the numerical simulations indicated that, for the three objects with small A/M values, solar radiation pressure causes small variations in the eccentricity and inclination. Also, as is clear from Figs. 1a, 2a, 3a, 1b, 2b and 3b the difference in A/M values led the objects to different evolutionary paths. The amplitude of the variation increases with the increase in the ratio A/M. In order to explore the problem when the ratio A/M takes large values, we carried out numerical simulations in two selected cases $A/M = 1$ and 0.02. Figs. 4a and 4b depict the long-term dynamical evolution of orbital eccentricity and inclination, in both cases, of the object with semi-major axis $a = 38678.878 \, km$. We observe from the Figs. dramatic differences between the two cases caused by solar radiation pressure, these differences increase as the ratio A/M takes larger values. To compare the effect of the considered perturbations, we represent the motion of the eccentricity and inclination in two cases: $J_2 - J_4$ and $J_2 - J_4 + SRP + Sun + Moon$, for a piece of debris with $A/M = 0.009$ in Fig. 5a and Fig. 5b. We found that the amplitude of variation is

dependent on the zonal potential and mainly on the solar radiation pressure. The motion of space debris is dominated by these two effects, while the effects due to the Sun and the Moon perturbations are small compared to the zonal potential and SRP. As the area-to mass ratio increases the solar radiation pressure will dominates strongly the dynamics of the problem. The current work dealt with the long-term dynamics of space debris orbits, via optical observations, under the influence of natural perturbations. We studied the long-term evolution of these objects to know the behavior of the population in the near future and to avoid its dangerous effects on operational satellites. Also one of our goals is to use the present semi-analytical technique to propagate thousands of space debris. The results showed that, in the selected range of A/M, the eccentricity and inclination have significant differences. While, in the case of large area-to mass ratio the amplitude variation in eccentricity and inclination will increase dramatically. It is obvious that, the dynamics of space debris at these altitudes is mainly governed by zonal potential and solar radiation pressure. The results are helpful to promote uncatalogued space objects observation and identification.
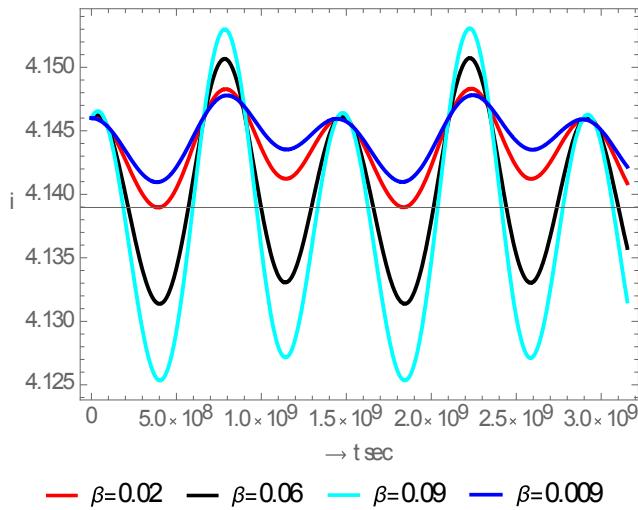

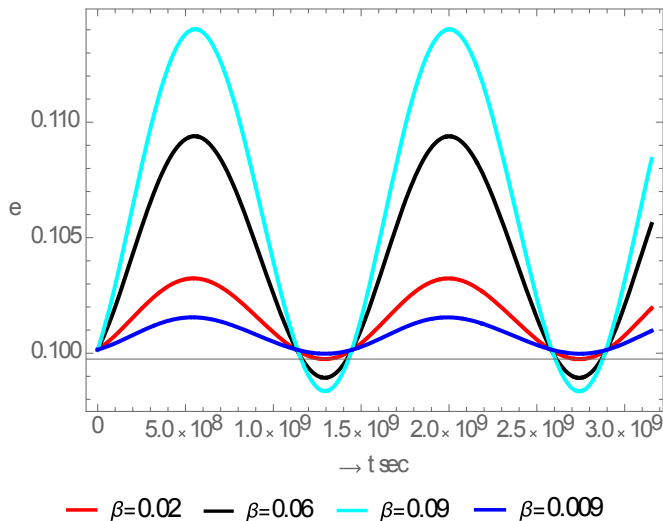Fig. 1a: Time history of inclination with different A/M. $a = 37025.652\ km$

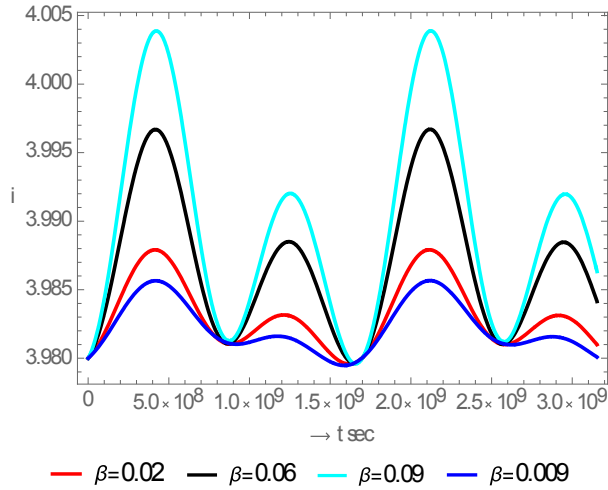Fig. 1b: Time history of eccentricity with different A/M. $a = 37025.652\ km$

Fig. 2a: Time history of inclination with different A/M. $a = 38978.878\ km$
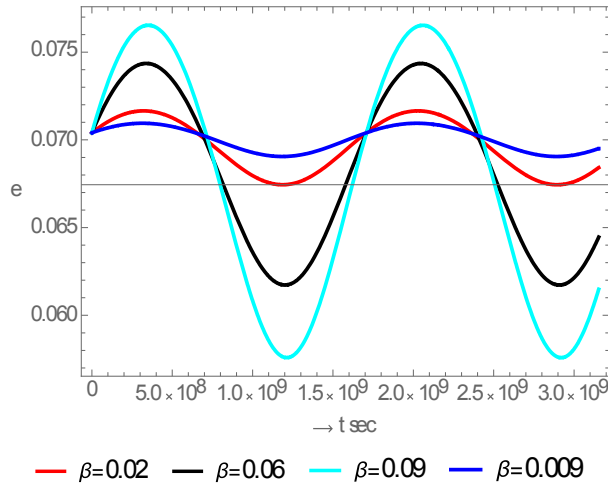

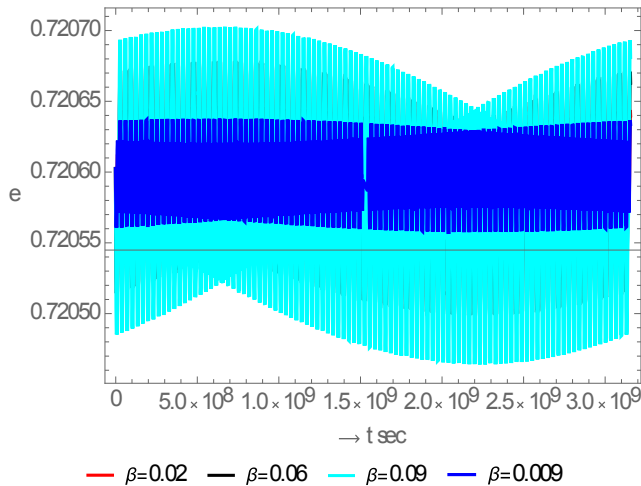Fig. 2b: Time history of eccentricity with different A/M. $a = 38978.878\ km$

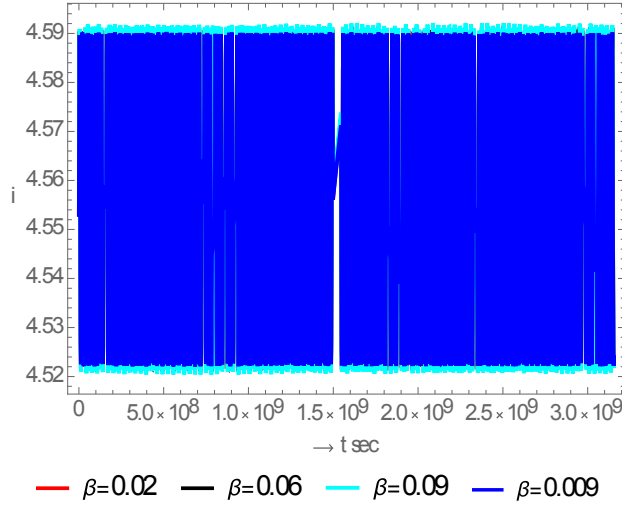Fig. 3a: Time history of eccentricity with different A/M. $a = 18863\ km$

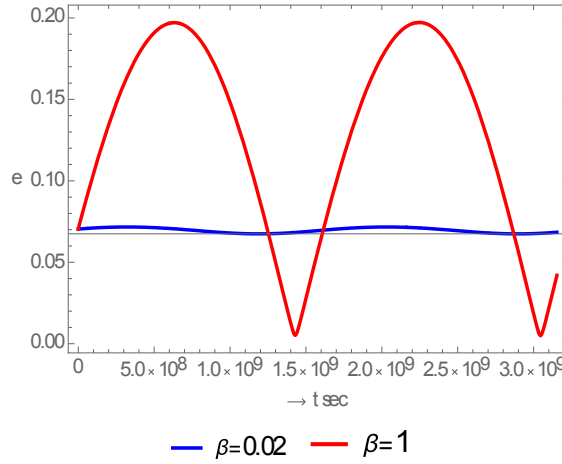Fig. 3b: Time history of inclination with different A/M. $a = 18863\ km$

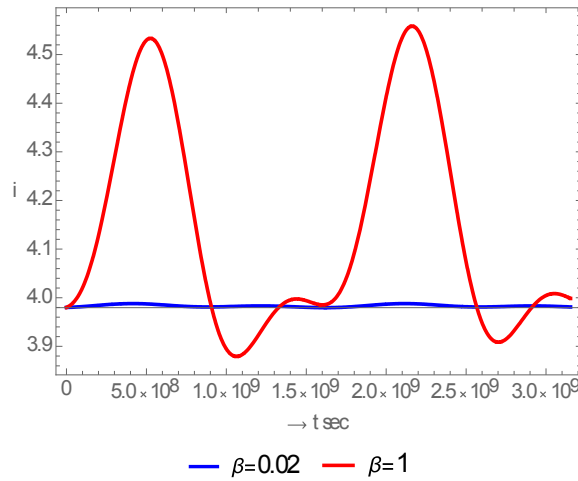Fig. 4a Long-term evolution of eccentricity, a $= 38678.878\ km$

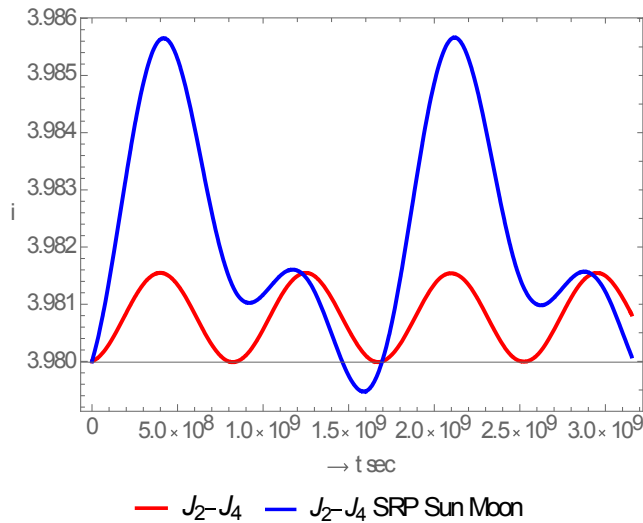Fig. 4b Long-term evolution of inclination, a $= 38678.878\ km$

Fig. 5a Comparison between two different models, $\beta = 0.009$, $a = 38678.878\ km$
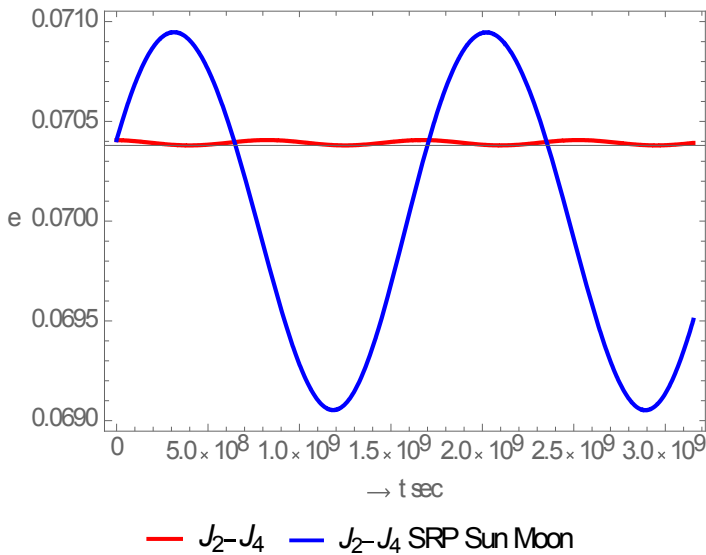

Fig. 5b Comparison between two different models, $\beta = 0.009$, $a = 38678.878\ km$

REFERENCES

[1] D. Casanova, C. Tardioli and A. Lemaître, Space debris collision avoidance using a three-filter sequence, *Monthly Notices of the Royal Astronomical Society,* vol. **442**, pp. 3235-3242, 6 2014.

[2] C. Bombardelli, Analytical formulation of impulsive collision avoidance dynamics, *Celestial Mechanics and Dynamical Astronomy,* vol. **118**, pp. 99-114, 2 2014.

[3] J. L. Gonzalo, C. Colombo and P. Di Lizia, Analytical Framework for Space Debris Collision Avoidance Maneuver Design, *Journal of Guidance, Control, and Dynamics,* vol. **44**, pp. 469-487, 2021.

[4] A. J. Rosengren, D. K. Skoulidou, K. Tsiganis and G. Voyatzis, Dynamical cartography of Earth satellite orbits, *Advances in Space Research,* vol. **63**, pp. 443-460, 2019.

[5] D. Casanova, A. Petit and A. Lemaître, Long-term evolution of space debris under the J_2effect, the solar radiation pressure and the solar and lunar perturbations, *Celestial Mechanics and Dynamical Astronomy,* vol. **123**, pp. 223-238, 10 2015.

[6] Y. Wang, X. Luo and X. Wu, Long-term evolution and lifetime analysis of geostationary transfer orbits with solar radiation pressure, *Acta Astronautica,* vol. **175**, pp. 405-420, 2020.

[7] S. Valk, A. Lemaître and L. Anselmo, Analytical and semi-analytical investigations of geosynchronous space debris with high area-to-mass ratios, *Advances in Space Research,* vol. **41**, pp. 1077-1090, 2008.

[8] Y. Abdel-Aziz, A. M. Abdelaziz, S. K. Tealib, G. F. Attia, I. Molotov and S. Schmalz, First Optical Satellite Tracking Station (OSTS) at NRIAG-Egypt, vol. **77**, p. 101361, 5 2020.

[9] J. Šilha, Space Debris: Optical Measurements, in *Reviews in Frontiers of Modern Astrophysics: From Space Debris to Cosmology*, P. Kabáth, D. Jones and M. Skarka, Eds., Cham, Springer International Publishing, 2020, pp. 1-21.

[10] R.-Y. Sun and C.-Y. Zhao, A new source extraction algorithm for optical space debris observation, *Research in Astronomy and Astrophysics,* vol. **13**, pp. 604-614, 5 2013.

[11] D. Hampf, P. Wagner and W. Riede, Optical technologies for the observation of low Earth orbit objects, *arXiv: Instrumentation and Methods for Astrophysics,* 2015.

[12] T. Schildknecht, Optical surveys for space debris, *The Astronomy and Astrophysics Review,* vol. **14**, pp. 41-111, 1 2007.

[13] D. Hampf, W. Riede, G. Stöckle and I. Buske, Ground-based optical position measurements of space debris in low earth orbits., in *Deutsche Luft- und Raumfahrtkongress*, 2013.

[14] S. Valk and A. Lemaître, Semi-analytical investigations of high area-to-mass ratio geosynchronous space debris including Earth's shadowing effects, *Advances in Space Research,* vol. **42**, pp. 1429-1443, 2008.

[15] S. Valk, A. Lemaître and F. Deleflie, Semi-analytical theory of mean orbital motion for geosynchronous space debris under gravitational influence, *Advances in Space Research,* vol. **43**, pp. 1070-1082, 2009.

[16] A. Lemaître, N. Delsate and S. Valk, A web of secondary resonances for large A/m geostationary debris, *Celestial Mechanics and Dynamical Astronomy,* vol. 104, pp. 383-402, 8 2009.

[17] C. Hubaux and A. Lemaître, The impact of Earth's shadow on the long-term evolution of space debris, *Celestial Mechanics and Dynamical Astronomy,* vol. **116**, pp. 79-95, 5 2013.

[18] C. Hubaux, A.-S. Libert, N. Delsate and T. Carletti, Influence of Earth's shadowing effects on space debris stability, *Advances in Space Research,* vol. **51**, pp. 25-38, 2013.

[19] A. V. Devyatkin, D. L. Gorshanov, V. V. Kouprianov and I. A. Verestchagina, Apex I and Apex II software packages for the reduction of astronomical CCD observations, *Solar System Research,* vol. **44**, pp. 68-80, 2 2010.

[20] D. A. Vallado, *Fundamentals of astrodynamics and applications*, 2nd ed. ed., Dordrecht; Boston: Kluwer Academic Publishers, 2001.

[21] J. P. Vinti, *Orbital and Celestial Mechanics*, G. J. Der and N. L. Bonavito, Eds., American Institute of Aeronautics and Astronautics, Inc., 1998.

[22] C. Colombo, Long-Term Evolution of Highly-Elliptical Orbits: Luni-Solar Perturbation Effects for Stability and Re-entry, *Frontiers in Astronomy and Space Sciences,* vol. **6**, p. 34, 2019.

[23] C. D. Murray and S. F. Dermott, *Solar System Dynamics*, Cambridge University Press, 2000.

[24] S. Belyanin and P. Gurfil, Semianalytical Study of Geosynchronous Orbits About a Precessing Oblate Earth Under Lunisolar Gravitation and Tesseral Resonance, *The Journal of the Astronautical Sciences,* vol. **57**, pp. 517-543, 7 2009.

[25] E. M. Alessi, G. Schettino, A. Rossi and G. B. Valsecchi, Solar radiation pressure resonances in Low Earth Orbits, *Monthly Notices of the Royal Astronomical Society,* vol. **473**, pp. 2407-2414, 10 2017.

[26] A. V. Krivov, L. L. Sokolov and V. V. Dikarev, Dynamics of Mars-orbiting dust: Effects of light pressure and planetary oblateness, *Celestial Mechanics and Dynamical Astronomy,* vol. **63**, pp. 313-339, 9 1995.

[27] T. Flohrer, H. Krag, H. Klinkrad and T. Schildknecht, Feasibility of performing space surveillance tasks with a proposed space-based optical architecture, *Advances in Space Research,* vol. **47**, pp. 1029-1042, 2011.